Survey of Magnesium Morphology in Chill Sample Castings Used for Spectrometer Analysis

Haruki Itofuji
I2C technology Institute, Ube City, Japan

Masayuki Itamura
Formerly, Tohoku University, Sendai, Japan

ABSTRACT

Previous studies have found that magnesium (Mg) exists as halo-like distribution around graphite in slowly cooled sample castings. In this study, Mg distribution in a rapidly cooled sample casting (with a mixed structure of ledeburite (chill) and graphite nodules) was surveyed by electron probe microanalysis (EPMA). Before EPMA, the sample contained free Mg and inclusion Mg using emission spectrometry. Two kinds of surface conditions were tested during the EPMA analysis. One was a hand-polished surface using diamond paste. The other was a milled surface by focused ion beam (FIB). Magnesium segregation was detected at voids, and across an entire section of sphere graphite nodules for both cases. The reasons why they exist there are based on Mg characteristics and the mechanism of spheroidal graphite (SG) formation. Here, the formation mechanism on the Mg halo is reviewed and the schematic illustration is introduced. Site theory, which was proposed as the graphite spheroidization theory in 1996 by the author, will be further investigated the next step.

Keywords: focused ion beam, FIB, electron probe microanalysis, EPMA, mapping analysis, Mg contained white iron, free Mg, castings

INTRODUCTION

In the past (circa 1950's) only optical microscopy (OM) had been used to observe graphite structure at the early stages. Since then, Scanning Electron Microscopy (SEM), Electron Probe Microanalysis (EPMA), Color Mapping Analysis (CMA), Transmission Electron Microscopy (TEM), Auger and Time-of-Flight Secondary Ion Mass Spectrometry (TOF-SIMS) have been used, and precise observation and analysis are now possible. Although many theories have been proposed on the nucleation and growth mechanism of spheroidal graphite, they have been categorized into two theories up to present.

One theory is the nucleus theory for SG nucleation[1-5] where graphite nucleates on substances. After nucleation, graphite grows to spheroidal graphite taking the spiral growth manner,[4,5] or while being influenced surface energy[1-3] as the final form. Nucleus theory as the graphite spheroidization theory has been supported by most researchers and metallurgical engineers at present. Doru. Stefanescu reviewed that the nucleus in spheroidal graphite and growth manner on it were revealed by recent electron microscopy studies.[6] Other researchers have reported that graphite nucleates at nucleus substance and grows to spheroidal form by surface tension accompanied by interfacial energy. In their papers, their model of growth manner and substructural evidence was insufficient. [1-3] There have been examples to adopt nucleus theory in the foundry.[7,8] However, their theory has not been easy to show as a clear effect for better quality in castings, and hard to adopt in foundry practice directly as a specific technology. For example, three-dimensional (3D) filters are necessary to capture both macro floating on and micro suspending inclusions in molten irons as the indispensable technology in current casting design and show superior effects for both microstructural and mechanical qualities of castings. It is known that macroinclusions are mechanically entrapped, and microinclusions are entrapped at the interfacial site between molten iron and filter surface as precipitation.[9-11] Here, microinclusions ironically are indispensable ones as the nucleus to form spheroidal graphite in nucleus theory. According to nucleus theory, filtration might be an anti-action for spheroidization. This contradiction point should be resolved for casting designers.

Another is site theory in which nucleation and growth can be explained by single theory.[12-14] The origin was gas bubble theory.[15] It is not popular among researchers, engineers and metalcasters yet. However, the site theory has been gradually gaining accepted in the foundry because phenomena during the production of ductile iron castings are easy to understand and engineers can take the specific technology to improve the quality of castings. There are many demonstrations and their applications as specific technologies by comprehending phenomena through site theory (examples are listed in Table 1).[16-43] Recent studies by combination with NF theory, authors have succeeded in getting full graphite structure in as-cast condition by both PM[18,22-24,33-36] and semi-solid (Rheo) casting.[21,24]

There are some phenomena which cannot be explained satisfactorily by site theory yet, like the role of Mg inclusion. This is an insufficient part to demonstrate in foundry practice still now. There are many followers of nucleus theory. In this study, the state of existence on Mg morphology like free Mg (MgF) and Mg inclusion (MgI) in rapidly cooled chill sample castings were surveyed using EPMA. From the results, the formation mechanism of Mg halo[14] was considered. The good relation of MgF with graphite nodularity and tensile properties has already been published.[16] Furthermore, the possibility of Mg inclusion to spheroidal graphite formation was also considered.

Table 1. Understanding Graphite Spheroidization through Site Theory[12-14] and Practical Application as Specific Technologies

No.	Items	Comprehension through Site theory	Demonstrations and applications	Reference
1	Role of Mg	・MgF takes main role.	・Found good relation of MgF with nodularity and tensile properties, inclusion did not. ・Demonstrated MgF analysis by spectrometer.	16
		・MgI is not really necessary for every graphite nodule.	・Found no relation of MgI with both nodularity and tensile properties.	
		・MgF exists as gas bubbles in molten iron.	・Demonstrated voids as trace of Mg gas bubbles in rapid cool chill samples.	17,18 This study
			・Demonstrated Mg halo around SG as the trace of gas bubblen in sand castings.	19,20
		・Gr. nucleates and grow in Mg gas bubbles.	・Detected Mg at whole section of SG in PM castings. ・Proposes formation mechanism of Mg halo.	This study
		・MgI do not take main role for graphite nucleation and growth.	・Demonstrated only 10% number of nodules contain Mg inclusion and such SG have also Mg halo.	21-24
		・Sphere graphite is the initial form for both SG and CVG. Poorer impurrity leads it to CVG.	・Demonstrated CVG starting to grow from sphere graphite and growth along filmy liquid chunnel which formed by impurity.	25
		・When the number of SG at early stage of solidification is a small, CG starts to form.	・Demonstrated CHG forming with no direct relation to preexisted SG at thermal center of castings.	26,27
2	Relation to CVG & CHG	・All formation mechanism should and could be explained with a single theory.	・Demonstrated the possibility to explain the mechanism of SG, CVG and CHG with same theory.	13,14,26 28
3	Substructure	・Every graphite morphology depends on the site where one graphite nucleates and grow. ・Their basic manner is based on graphite crystal structure and never changed by external factors.	・SG, CVG and CHG have poly crystal structure consisting with graphite chips. ・They have basically the same substructure.	28
4	Expansion force	・Verified the amount of Gr. precipitation during solidification was the same even if different modulus.	・Have same amount of Gr precipitation in solidification regardless the size of castings.	29
		・Since Mg gas bubble are used for Gr formation, when the number of Gr nodule is large, growth per nodule is less and expansion force is small.	・Demonstrated that force in smaller castings was lower than that of larger castings.	30
			・Developped heat ballancer as a kind of riser.	31
		・Under high pressure, Mg gas bubble disappear and liquidize. SG does not form in this case.	・Found excessive chills made solidification temperature range rose up and promoted formation of CHG.	29
			・Found that chills should not use at least one of mold surface to avoid CHG.	
5	Inoculation	・One of aims is to introduce Si density spots into molten iron.	・Demonstrated Si map by using EPMA as the evidence of density spots.	19
		・Another is to make NF harmless and not to make Fe_3C formation active.	・Developed Chill-free PM casting method by controlling NF.	21,33-36
6	Acuracy of CAE analysis	・Volumetric change should be considered according to Fe-C phase diagram and cooling curve.	・Developed shrinkage analysis soft taking equilibrium amount of contraction and expansion and their timing.	37-39
7	Enbrittlement at 400℃	・Mg_3C_2 forms among eutectic cells under stress and may make materials brittle.	・Found canceling extra MgF among eutectic cells by Phosphorus.	40
8	All joined	・Required and aimed quality in castings can be produce intentionally.	・ Guaranteed mechanical properties in castings .	21,32-36, 41-43

【Note】
Gr.; Graphite, CVG; Compacted vermicular graphite, CHG; Chunky graphite, NF; Atomic nitrogen = Free nitrogen

EXPERIMENTAL PROCEDURE

Magnesium morphology in chill sample castings, which are used in daily foundry practice for chemical analysis, was surveyed. At first, chemical composition was analyzed using an emission spectrometer in conjunction with pulse height distribution (PDA) system. This spectrometer is possible to analyze residual (total) Mg (MgT), inclusive Mg (MgI), and free Mg (MgF) which is atomic morphology and no bonding with other elements.[16] The analysis mechanism is the same as acid-soluble aluminum (Al) and insoluble Al in steelmaking, basically.[44] After spectrometer analysis, the spark trace was observed using SEM to check the condition of luminescence excitation. A two inch Y-type sample was poured into a furan sand mold from the same heat. Then, practical casting products, which are rough weight of 870kg, were poured. The material grade was designed to be ASTM A536 65-45-12. Secondary, chill sample castings were analyzed using EPMA with a color mapping analysis (CMA) system. Two kinds of analyzed surfaces were prepared. One was polished with diamond paste, and another was milled using FIB. The latter was conducted to confirm that inclusions might not be dropped out from matrix by polishing and the results in the first CMA analysis. The FIB condition is shown in Table 2. Both surfaces were observed and analyzed using CMA. The conditions are shown in Table 3.

Table 2. Condition of FIB Processing

Steps of Milling		Beam Φ(μm)	Current (μA)	Time (min.)
Rough		500	23.535	60
Intermediate finish	1st	300	8.545	10
	2nd	100	0.854	10
Finish	1st	50	0.161	10
	2nd	50	0.034	30

Table 3. Condition of EPMA Mapping Analysis on Mg

Items	Surface preperation	
	Hand polished	FIB milled
Acceralte voltage (kv)	15	15
Irradation current (A)	3.10E-07	3.01e-07A
Beam diameter (μm)	0.26	0.26
Dwelling time (μs)	50	50
Points (X , Y)	450x450	200x200
Method	WDS	WDS
Spectrum crystal	TAP	TAP
Scanning	Stage	Stage

RESULTS

The analytical results of chemical composition by emission spectrometer are shown in Table 4. The sparking traces are shown in Figs. 1 and 2. Even if inclusions are contained in graphite nodules, such inclusions could be said to be analyzed all from judging sparking trace (Fig. 2-B).

Table 4. Chemical Composition (mass%)

C	Si	Mn	P	S	Ce	MgT	MgI	MgF
3.49	2.41	0.16	0.031	0.014	0.008	0.0480	0.0075	0.0405

Table 5. Tensile Properties

$\sigma_{0.2}$ N/mm²	σ_B N/mm²	ε %	Φ %	Brake
308	471	25	23	A
313	472	27	23	A
324	490	18	13	A
324	496	21	12	A

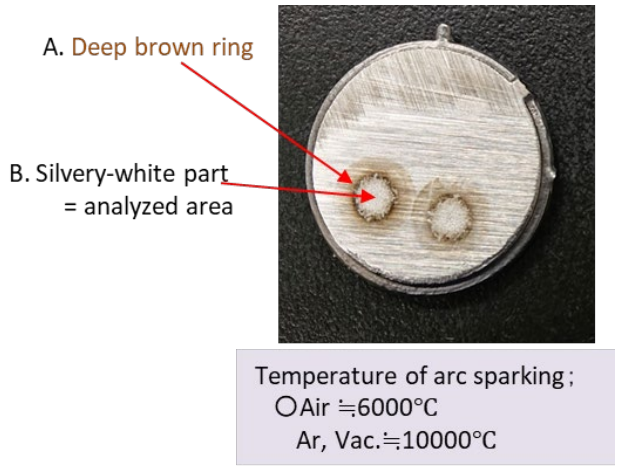

Figure 1. Sparking trace by spectrometer.

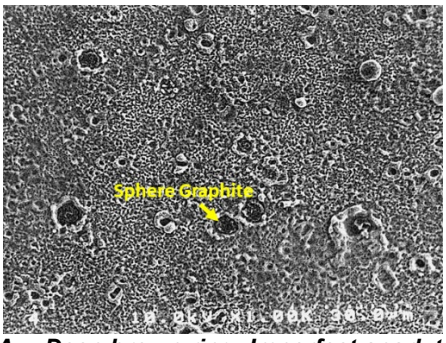

A. Deep brown ring; Imperfect spark trace.

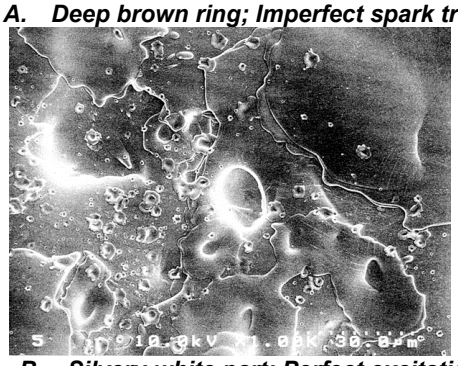

B. Silvery-white part; Perfect excitation.

Figure 2. SEM photos of sparking trace.

The results of tensile tests were good as shown in Table 5. Casting products had no problem with quality. Chemical composition is as practical values except the indication of MgI and MgF. An SEM-comp photo of the polished surface is shown in Fig. 3. Although sample castings were poured and chilled in permanent mold (PM), SG forms usually. However, it did not influence the analytical results, as already shown above. It will be better to have as small a number as possible in precise analysis. The results of the CMA analysis on the polished surface are shown in Fig. 4.

Magnesium was detected at sphere graphite nodules, inclusions, and voids. Such voids are considered as traces of Mg gas bubbles according to the former study.[17] Several sphere graphite nodules were observed using SEM. The results are shown in Fig. 5. They were the size of ~2–3μm and had no inclusions in their bodies. Ledeburite cementite behind some nodules is seen through. They are not inclusive substances in graphite nodules.

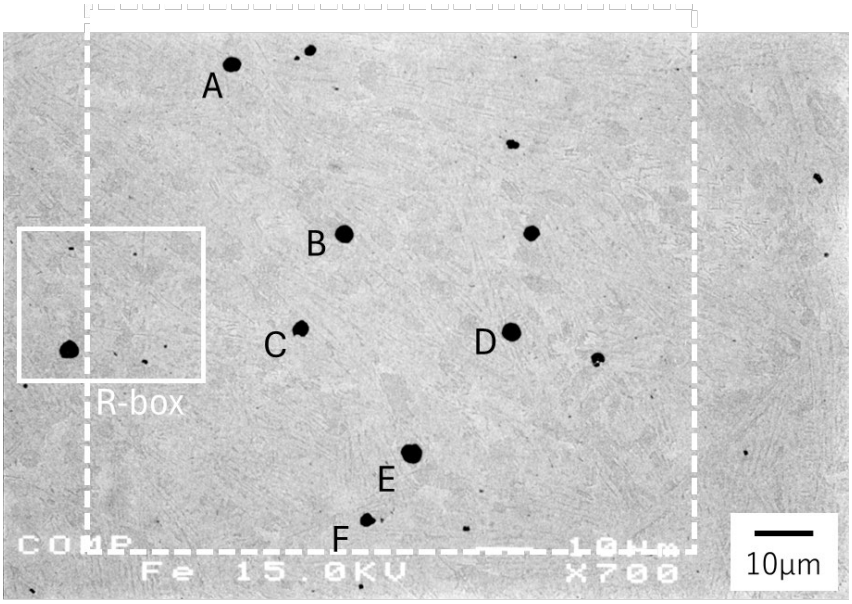

Figure 3. SEM-COMP photo of analysis surface; Dashed line square = Mapping, Line square = EDS.

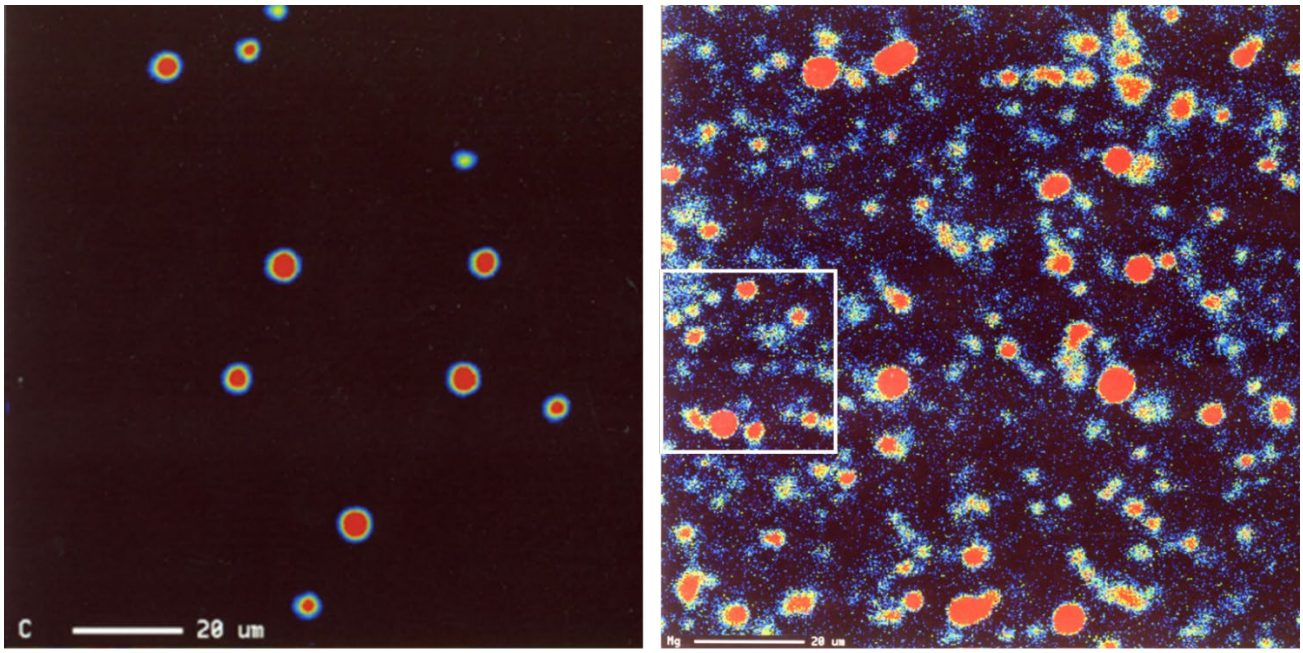

a. C-Map b. Mg-Map

Figure 4. Results of mapping analysis; red is highest, and black is lowest.

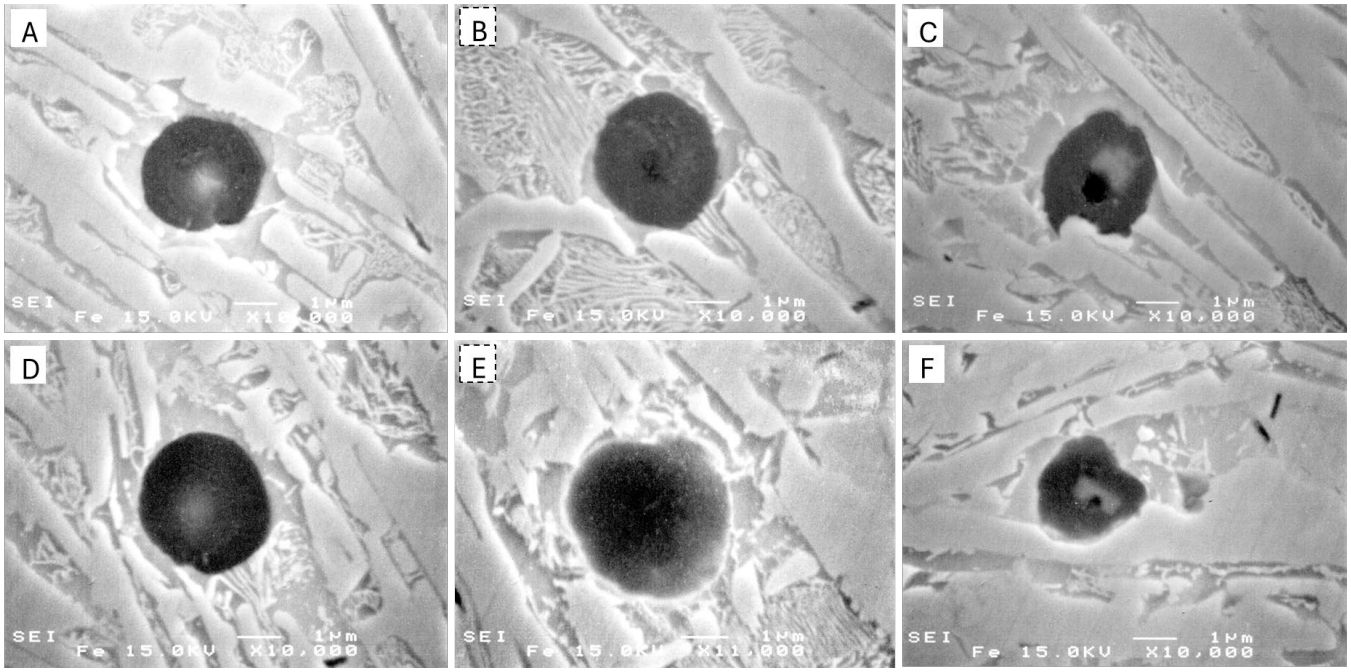

Figure 5. SEM photos of sphere graphite A–F shown in Fig. 3.

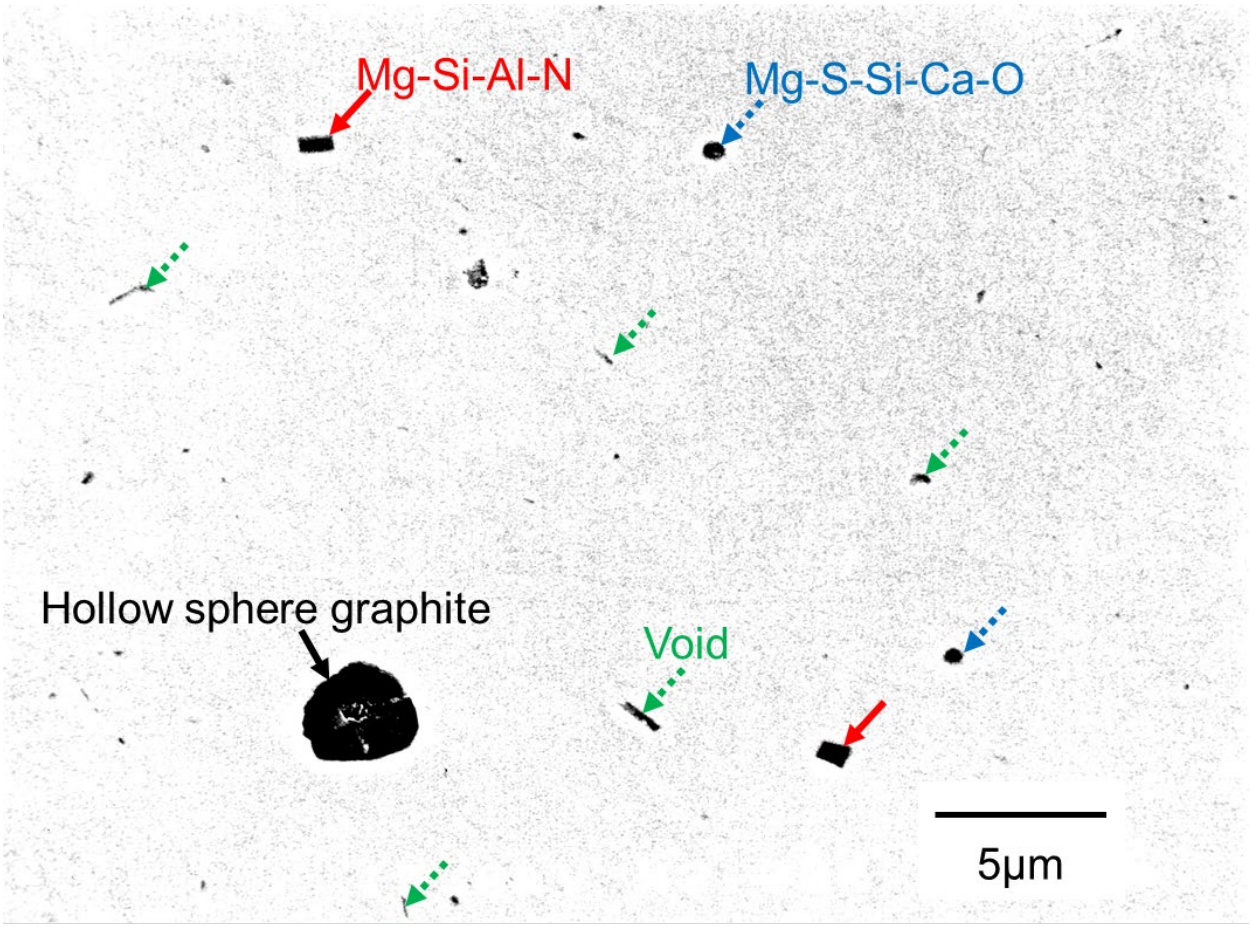

Figure 6. SEM-COMP photo from the R-box area shown in Fig. 3; rectangles = nitride, round spots = oxide, others without arrow = voids.

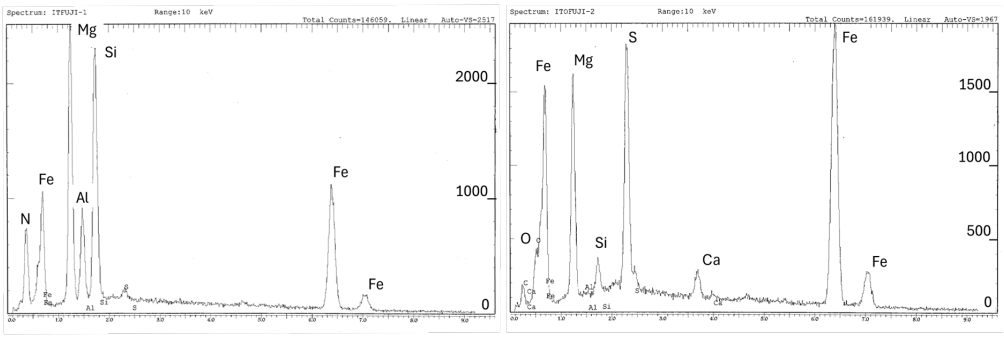

a. Mg-Si-Al-N system rectangular inclusion b. Mg-S-Si-Ca-O system Nodular inclusion

Figure 7. The results of XRD analysis at inclusions in R-box shown in Fig. 3.

The results of SEM-COMP observation and X-ray diffraction (XRD) analysis of inclusions within the square box in Fig. 3 are shown in Figs. 6 and 7, respectively. Rectangle-like inclusions were Mg-Si-Al nitride and spheroidal formed inclusions were Mg-Si-Ca oxy-sulfides. Other black spots were voids as the trace of Mg gas bubbles. During the process of ledeburite formation in solidification, it will be supposed that needle-like structures make bubbles deform. The existence of voids will be clear by another CMA analysis later. Spheroidal graphite containing inclusions was not observed in the area shown in Fig. 2, but such a SG was observed in a few cases in the other area. However, the shape of such nodule was not spheroidal, but deteriorated. This seemed to be the same as most researchers have reported.[1-5] The example is shown in Fig. 8. If Mg inclusions take a key role for graphite spheroidization, more SG should contain inclusions but did not in fact.

The surface of FIB milling is shown in Figure 9. Milling was conducted from the top down in the figure. Vertical lines show milling flows. The flow is marked when there is graphite or an inclusion in the direction of milling. SG contained inclusion was not observed around milling area. Since the size of sphere graphite observed in this study and nuclei reported by other researchers were the same as ~2–3µm a greater number of nodules should contain in graphite bodies in Figs. 2 and 9. However, it was not, in fact.

Another CMA analysis was conducted within the area of square A shown in Fig. 9. A higher magnification SEM photo is shown in Fig. 10a. The results are shown in Fig. 11. Magnesium distribution was detected at SG and voids the same as the first CMA analysis. The existence of voids was confirmed within square B shown in Fig. 10a. The higher magnification of the SEM photo at square B is shown in Fig. 10b. Voids exist, and they are not a trace of dropping off inclusion because of the surface preparation by FIB milling.

CONSIDERATION

In former studies,[16,17] the existence of MgF was demonstrated by spectrometer, and CMA mapping analysis, and furthermore the good relationship between MgF and not only tensile properties but also graphite nodularity was found. In the case of chemical analysis, it was pointed out by researchers that Mg inclusions in graphite nodules might not be analyzed because graphite did not resolve acid.

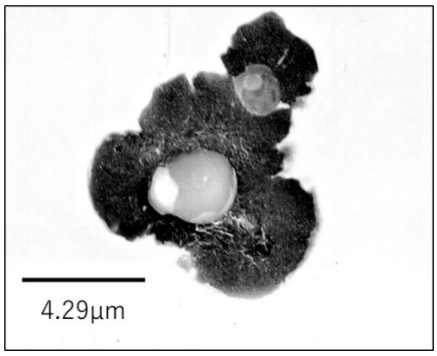

Figure 8. An FE-SEM photo of deteriorated SG with inclusions.

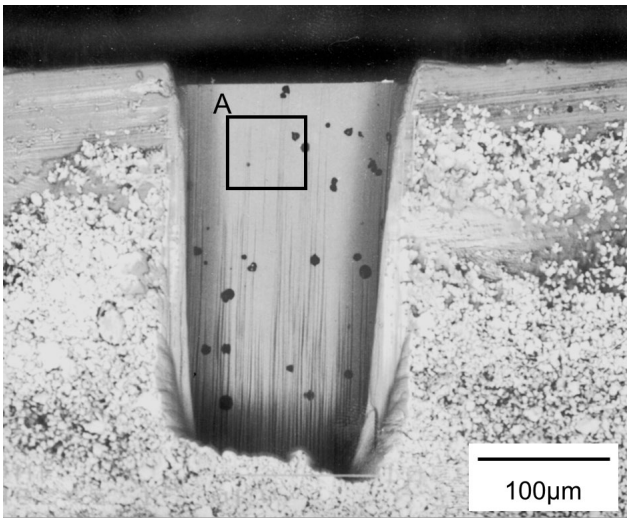

Figure 9. The SEM photo of the FIB milling area.

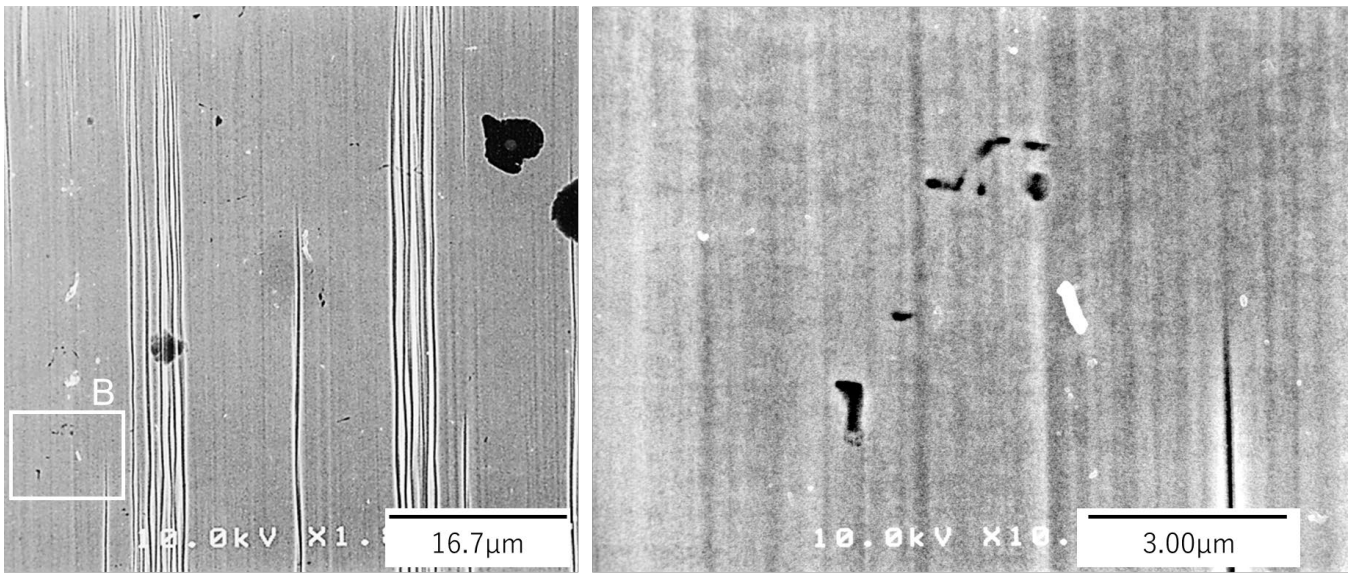

a. Area of CMA analysis. ***b. High magnification in square B.***

Figure 10. SEM photos of the milling surface.

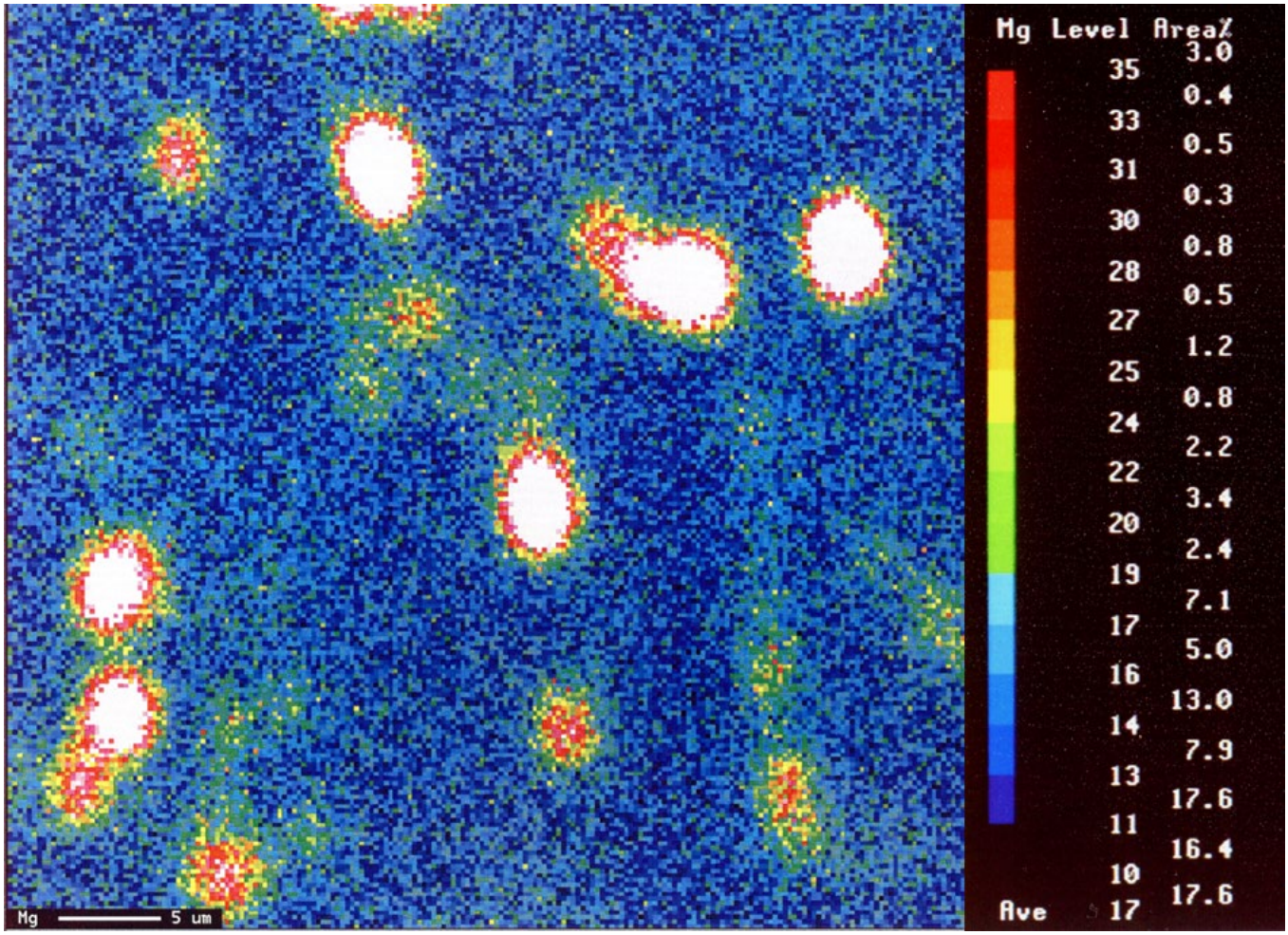

Figure 11. Result of Mg mapping analysis using CMA; White area is a level of over thirty-five.

This was cleared soon because graphite nodules extracted electrolytically were easily decomposed by ultrasonic vibration in analysis process.[13,26] If inclusions are contained in graphite nodules, they will be released into electrolyte and resolved by acids for ICP analysis.[16] The same was true for spectrometer analysis that everything including the graphite was fused by luminescence excitation. This was demonstrated in this study.

The author has concluded in a previous paper[17] that MgF was the trace of gas bubbles and existed as voids in chill sample castings. However, it was pointed out that Mg inclusion dropped out by polishing and made voids. This was cleared by FIB milling in this study that Mg voids exist, in fact. The experimental facts, that Mg contained chill sample castings can be graphitized in shorter time by heat treatment than that of Mg non-contained ones because of the existence of voids as free surface,[18,45-46] support this.

Inclusions are simply considered substances as the results of deoxidation and desulfurization in molten irons. However, more studies will be needed to complete.

The author found Mg halos considered as trace of gas bubbles around graphite nodules.[12-14,19,20] However, it was not in this study. Magnesium distribution might change its position during the formation process considering basic crystal structure, substructure of spheroidal graphite, and atomic and crystal size of Mg (Fig. 12), in addition to the results in this study. Magnesium atoms might possibly exist between graphite layers in graphite nodules before their solidification. However, after Mg forms crystal structure by solidification, Mg will be quite difficult to exist between graphite layers because the crystal size is too big. The guessable mechanism of Mg halo formation is shown in Fig. 13.

CONCLUSION

As the results of the morphological survey on Mg-contained chill sample castings, the following conclusions were made clear.

1. Mg contained chill sample castings could be analyzed morphologically in practice operation and sorted into free Mg (MgF) and Mg inclusions (MgI).
2. There were voids, sphere graphite nodules and rarely inclusions on the analyzed surface.
3. Free Mg was detected from voids and sphere graphite nodules. They were considered traces of Mg gas bubbles.
4. MgF is a key factor and necessary for the control of graphite spheroidizing and production in SGI castings.
5. Inclusions might play a subordinate role in the formation of spheroidal graphite.

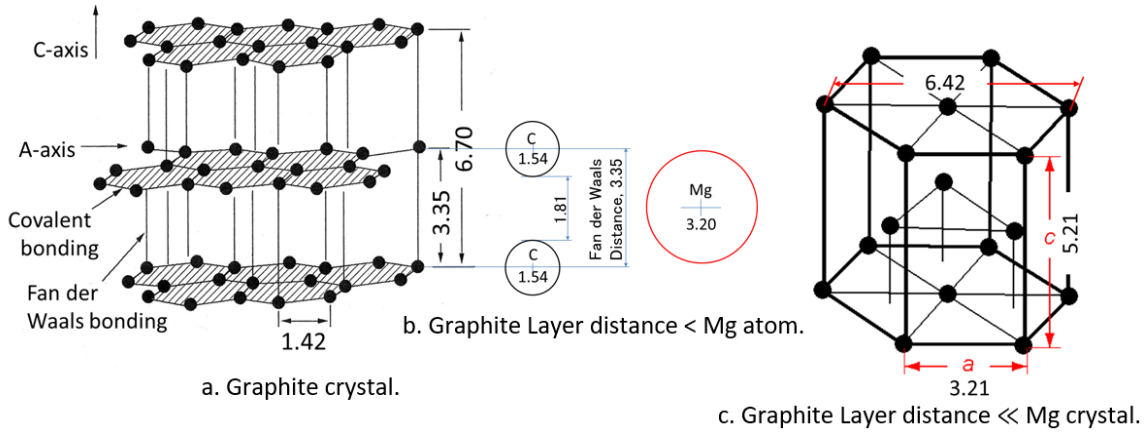

Figure 12. Relation of atomic and crystal size between SG and Mg; Unit Å.

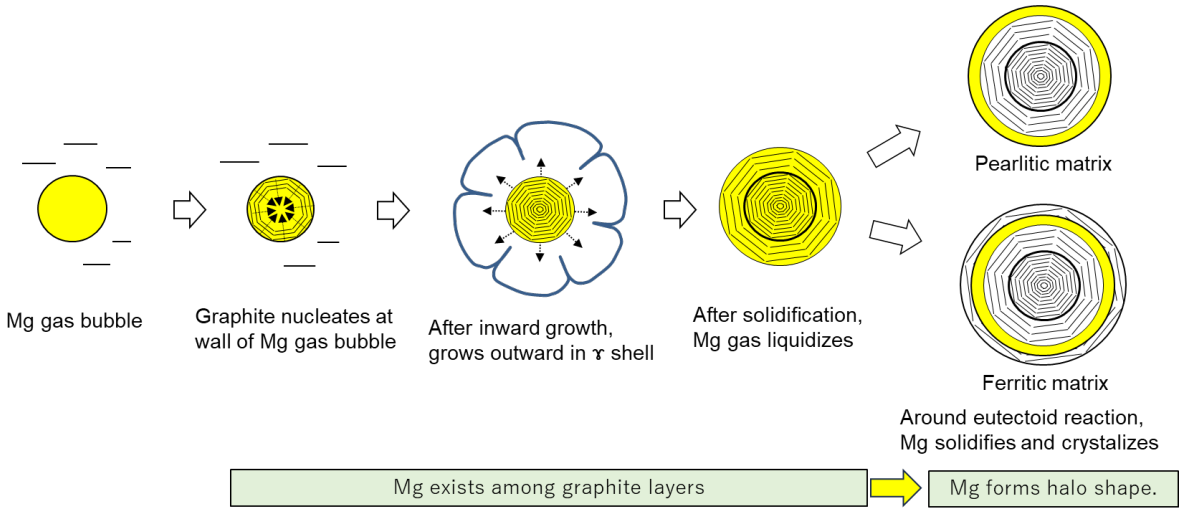

Figure 13. The schematic mechanism of Mg halo formation in SGI.

REFERENCES

1. A. Pugliara, L. Laffont, T. Hungria, J. Lacaze, "3D-STEM Observation of a Multiphase of Spheroidal Graphite," *2nd Carl Loper Cast Iron Sympo* (2019).
2. H. Nakae, Y. Igarashi, Y. Ono, "Heterogeneous Nucleus of Spheroidal Graphite and Mechanism of Spheroidal Graphite Formation," *J. JFS*, 73, 2 (2001) 111-117.
3. H. Horie, "Review on Nucleus and Mechanism of Spheroidal Graphite Formation in Cast Iron," *J. JFS* 90, 10 (2018) 560-568.
4. D. M, Stefanescu, G. Alonso, P. Larranaga, E. L. La Fuente, R. Suarez, "Reexamination of Cristal Growth Theory of Graphite in Iron-Carbon Alloys," *Acta Materialia*, 139 (2017) 109-121.
5. G. Alonso, B. Bravo, D. M. Stefanescu, R. Súarez, "Graphite Spheroids: The Place Where they are born," *Int. J. Metalcasting*, (Apr. 2024).
6. D. M. Stefanescu, G. Alonso, R. Suárez, T. Tokarski, M. Górny, "Growth Mechanism of Graphite Spheroids from Nano- to Micro-Scale," *Int. J. Metalcasting* (Jan. 2024).
7. Y. Igarashi, "Analysis of the Nucleus of Spheroidal Graphite and its Application to Production" Thesis of Doctor Degree in Waseda University (2004).
8. G. Alonso, J. R. Olaizola, D. Stefanescu, R. Súarez, "The Effects of Holding Time in the Heating/Pouring Unit on the Metallurgical Quality of Spheroidal Graphite Iron," *Int. J. Metalcasting* (Sept. 2022).
9. M. Ishibashi, "The Filtration of Cast Iron with Ceramic Foam Filters," *J. JFS* 62, 8 (1990) 607-614.
10. H. Sagawa, H. Itofuji, H. Uchikawa, N. Hashimoto, "Filtration effect in Tundish," *JIMM*, chu-shikoku, Branch, 31st Meeting (1990) p. 26.
11. I. A. Andrews, A. L. Matthews, "Molten Metal Filtration," *DIS, Ductile Iron News*, Issue No.1 (1999).
12. H. Itofuji, "Study on Graphite Spheroidization in Cast Irons," *Thesis of Doctor's Degree* in Kyoto University (1993).
13. H. Itofuji, "Proposal of Site Theory," *AFS Trans*., 104, (1996) 79-87.
14. H. Itofuji, "Mg Halo as Trace of Gas bubble in Spheroidal Graphite," *J. JFS*, 90, 10 (2018) 587-593.
15. S. Yamamoto, Y. Kawano, R. Ozaki, Y. Murakami, Mechanism of Nodularization of Graphite in Cast Irons Treated with Magnesium, *Metal Science*, 12, (May 1978) 239–246.
16. H. Itofuji, "The Influence of Free Magnesium on Some Properties in SGI," *Int. J. of Cast Metals Research*, 12, 3(1999) 179-187.
17. H. Itofuji, Study of Voids in Chilled Samples of Magnesium-Treated Irons, *Int. J. of Cast Metals Research*,17,4 (2004) 220-228.
18. K. Edane, K. Matsugi, H. Itofuji, Y. B. Choi, K. Sugio, K. Kambayashi," Decisive Difference between as Cast and Tempered Graphite Distribution in Permanent Mold Spheroidal Graphite Iron Castings," *Mat. Tra*. 66, (2025) MT-M2024117/awaiting publication.
19. H. Itofuji, "Magnesium Map of the Spheroidal Graphite Structure in DCI," *Cast Metals*, 5, 1 (1992) 6-19.
20. H. Itofuji, "A Detailed Study of the Site of Mg-Halo as Detected by CMA," *Int. J. of Cast Metals Research*, 14, 1(2001)15-23.
21. M. Itamura, H. Itofuji, M. Adachi," Spherical Graphite Cast Iron Semi-Solid Casting Method and Semi-Solid Cast Product," WO 2018/043685 A1, ar.8 (2018).
22. H. Itofuji, M. Itamura, K. Anzai, K. Yamaguchi," Method for Producing Die-Cast Product of Spheroidal Graphite Cast Iron Having Ultrafine Spheroidal Graphite and Die-Cast product of Spheroidal Graphite Cast Iron," US 11,254,993 B2, Feb.22 (2022).
23. H. Itofuji, M. Itamura, "Method for producing Die-Cast Product of Spherical Graphitic Cast Iron Including Ultrafine Spherical Graphite, and Spheroidizing Treatment Agent," US 11,845,999 B2, (Dec.19, 2023)
24. H. Itofuji, K. Edane, T. Sakatani, N. Utagawa, M. Itamura, "PM and Rheocasting in Ductile Iron Castings," *IJMC*, V.18 (May 12, 2024) 2036-2047.
25. H. Itofuji, Y. Kawano, N. Inoyama, S. Yamamoto, B. Chang, T. Nishi, "The Formation Mechanism of Compacted Vermicular Graphite in Cast Irons," *Trans. AFS*, 91(1983)831-84.
26. H. Itofuji, H. Uchikawa, "Formation Mechanism of Chunky Graphite in Heavy Section Ductile Cast Irons," *Trans. AFS*, 98 (1990) 429-448.
27. H. Itofuji, A. Masutani, "Nucleation and Growth Behavior of Chunky Graphite," *Int. J. of Cast Metals* Research, 14, 1(2001) 1-14.
28. H. Itofuji, Y. Kawano, S. Yamamoto, N. Inoyama, H. Yoshida, B. Chang, "Comparison of Substructure of CV Graphite with Other Types of Graphite," *Trans. AFS*, 91(1983)313-324.
29. T. Kotani, K. Edane, H. Kambayashi, K. Iwakado, H. Itofuji, "Amount of Free Carbon in SGI Castings with Different Modulus," *Trans. AFS*, 124 (2016) 215-219.
30. T. Kotani, K. Edane, H. Kambayashi, K. Iwakado, Y. Miyamoto, H. Itofuji, "Effect of Modulus on Solidification Expansion Pressure and Displacement in Spheroidal Graphite Iron Castings," *J. JFS*, V. 92, N. 4 (2020) 175-181.
31. K. Ishikawa, T. Kotani, T. Ogino, H. Itofuji, "Effect of Heat Balancer Technique applied for Heavy Section Ductile Iron Castings," *The 12th AFC* (2013) A1-1 00013.
32. H. Itofuji, Y. Miyamoto, K. Iwakado, T. Kotani "Examples of Chunky Graphite Formation in Production of Ductile Iron Castings and Effective

Countermeasure*," IJMC*, (May 17, 2024).
33. H. Itofuji, K. Edane, T. Kotani, M. Itamura, K. Anzai, "Ultrafine Spheroidal Graphite Iron Castings," *Material Transactions* 60,1(2019)41-48
34. H. Itofuji, K. Edane, T. Sakatani, M. Itamura, " Ultrafine Spheroidal Graphite Iron Castings by use of Thin-Walled PMs,"*2nd Carl Loper Cast Iron Sympo.* (2019) Oct 01.
35. H. Itofuji, Y. Miyamoto, M. Itamura, "Influence of Free Nitrogen on Tendency of Chill Formation in Spheroidal Graphite," *Mat Tra*. V62, N8(2021)1194-1202.
36. K. Edane, H. Itofuji, K. Matsugi, Y. B. Choi, H. Kambayashi," Quantitative Change of Nitrogen States in Melting Process for Permanent Mold Casting of Spheroidal Graphite Iron," *MatTra*, V64, N11 (2023) 2637 – 2642.
37. Y. Miyamoto, H. Itofuji, "Shrinkage Analysis Considering Expansion and Contraction Behavior in Heavy Section SGI Castings," *Trans. AFS*, 127 (2019) 243-250.
38. H. Itofuji, Y. Miyamoto, "Casting Solidification Analysis Method, Casting Method, and Electronic Program," US 11,745,258 B2 (Sept. 5, 2023).
39. Y. Miyamoto, H. Itofuji, "Shrinkage Analysis Considering Expansion and Contraction Behavior in Heavy Section Spheroidal Graphite Iron Castings," *AFS Metalcasting Congress* (2025) Paper #25-087.
40. H. Itofuji, A. Masutani, "Embrittlement at elevated temperature in Spheroidal Graphite Iron," *JSPS report* (2000) 283-295.
41. H. Itofuji, "Application of the Site Theory on the QC of Heavy Section SGI Cast Iron," *1st Keith D. Millis World Sympo.* (1993) 1-40.
42. H. Itofuji, K. Kiyonaka, "Guarantee of Mechanical Properties in Ferritic Spheroidal Graphite Iron Castings with Heavy Section," *J. JFS*, V.80, N2 (2008) 113-119.
43. H. Itofuji, M. Tamura, H. Ito, T. Nishimura, Y. Esashika, "Production of the 7-ton Nonmag. DI Castings for World Largest Class Power Generator," *MatTra*, V51, N1 (2010) 103-109.
44. K. Mizukami, M. Sugiyama, W. Ohashi, K. Mizuno," Identification of Acid Soluble Components and Acid Insoluble Inclusions in Spark OES Pulse Height Distribution Analysis," Shinnittetsu giho, 390 (2010) 67-75.
45. Y. Lee, Effects of Gasses, and gas elements on microstructural changes, in Cast Iron, *Thesis of Doctor Degree*, Kyoto University (1986).
46. Y. Miura, N. kashiwagi, Z. Motizuki, PM casting for grey iron, *JFS*, 359-371 (1976).